JCTC Journal of Chemical Theory and Computation

Article

pubs.acs.org/JCTC

Physicochemical Properties of Hazardous Energetic Compounds from Molecular Simulation

Alauddin Ahmed and Stanley I. Sandler*

Center for Molecular and Engineering Thermodynamics, Department of Chemical and Biomolecular Engineering, University of Delaware, Newark, Delaware 19716, United States

Supporting Information

ABSTRACT: A protocol is presented and used for the computation of physicochemical properties of nitroaromatic energetic compounds (ECs) using molecular simulation. Solvation and self-solvation free energies of ECs are computed using an expanded ensemble (EE) molecular dynamics method, with the TraPPE-UA/CHELPG and CGenFF/CHELPG force field models. Thermodynamic pathways relating Gibbs free energies and physicochemical properties are used to predict the room temperature vapor pressures, solubilities (in water and 1-octanol), Henry's law constants, and partition coefficients (octanol–water, air–water, and air–octanol) for liquid, subcooled, and solid ECs from the molecular simulations. These predictions are compared to experimental data where available. It is found that the use of the TraPPE-UA model with CHELPG charges computed here leads to predictions of measured physicochemical properties of comparable accuracy to that of other theoretical and empirical models. However, the advantage of the method used here is that with no experimental data, unlike other methods, a number of physicochemical properties for a compound can be calculated from only its atomic connectivity, charges obtained from density function theory (DFT), and choice of force field using two simulations: its self-solvation free energy and its Gibbs free energy in a solvent.

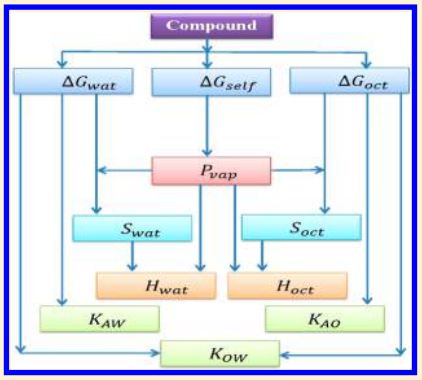

I. INTRODUCTION

Nitroaromatic energetic compounds (ECs), their intermediates during synthesis and their products during degradation, are toxic (metabolic and carcinogenic), mutagenic, and xenobiotic. The ECs are widely used in the military (as explosives and propellants), in industry (as solvents, dyes, and in polyurethane foams), in mining, in demolition, and in agriculture (as herbicides and insecticides). The most common forms of EC contamination are in surface and groundwater, in soil, and in sediment, due to air and water mediated solvation and transport. The ecological and biological impacts resulting from solvation in organic media, and atmospheric dispersion followed by inhalation, leads to the presence of the ECs in cells, the respiratory and nervous systems, the blood, and various organs.

Vapor pressures and Henry's law constants (HLC) are used in predicting air–water interphase exchange rates, which is important in the atmospheric transport.[1−4] The subcooled liquid vapor pressure is used to predict vapor–particle partitioning.[5−7] However, experimental data on subcooled liquid vapor pressures are extremely sparse in the literature, and especially so for energetic compounds. The vapor pressures of subcooled components are important because even though they are solids at room temperature, these compounds can be present in atmospheric aerosols and in gas-particle partitioning, and environmental models often use the subcooled liquid vapor pressure as a reference state. The experimental techniques used for the measurement of the vapor pressure of solids[8−13] cannot be used for a subcooled liquid; however, the subcooled liquid vapor pressure can be estimated from the vapor pressure of the solid using the measured enthalpy of fusion and melting point data.

Water solubility plays a central role in the ultimate fate of these energetic compounds in the environment as it determines the rate and extent of water mediated transport and the rates of biodegradation, hydrolysis, and oxidation.[14] The octanol–water partition coefficient (K_{OW}) is frequently used to correlate the behavior of xenobiotic ECs in the environment[15] and to predict some important quantities such as the bioconcentration and biomagnification[16] factors, soil–water sorption coefficients,[17] air–mammal tissue partition coefficients,[18] skin permeability,[19] nonspecific toxicity, metabolism, and effects on the central nervous system.[15,20−22] Also, the atmospheric transport of volatile compounds,[23,24] the surface–air distribution, the partitioning into the atmosphere and terrestrial organic phases, and bioaccumulation[25] have all been correlated with the octanol–air partition coefficient. Air–water (K_{AW}) and air–octanol (K_{AO}) partition coefficients are also used for describing absorption into an aerosol.[23,26−29]

The level of penetration of nitroaromatic residues on human skin or the presence of ECs in biota are also determined by their solubility in organic media. The molecular structure of 1-octanol, with a hydrophilic head and lipophilic tail, has resulted

Received: December 27, 2012
Published: March 12, 2013

   dx.doi.org/10.1021/ct301129x | J. Chem. Theory Comput. 2013, 9, 2389−2397

in it being used as a model solvent to approximately characterize many biological solvation processes.[30]

The free energy of solvation can be used to calculate physicochemical properties such as partition coefficients[31] (K_{OW}, K_{AW}, K_{AO}), Henry's law constants (HLC), solubilities,[32] vapor pressures,[33] rate constants,[34,35] and phase equilibria.[36] The most common experimental method of determining solvation free energy of a solute is from the ratio of its molar concentration in its pure gas phase to that in a liquid solvent at a specified composition.[37,38] Except for 2-NT and 3-NT,[39] solvation free energy data in water and 1-octanol for the ECs shown in Figure SF1 and listed in Table ST1 of the Supporting Information (SI) are unavailable in the literature.

The focus of this paper is to establish a thermodynamic framework for using solvation free energies computed from simulations to calculate the vapor pressure, solubility, Henry's law constant, and partition coefficients (K_{OW}, K_{AW}, K_{AO}) for species in the liquid, solid, and subcooled liquid states and to apply this procedure to the energetic compounds considered. Of particular interest are vapor pressures and solubilities in water and 1-octanol. We compute these here using expanded ensemble (EE) molecular dynamics simulations, published force fields, and partial charges computed from density functional theory.

II. METHODS

A. Theory. The solubility of a solute in a solvent can be computed from its solvation and self-solvation Gibbs free energies.[32] For a solute at room temperature, the Gibbs free energy needed to transfer a single molecule from its liquid or subcooled liquid to the gas phase can be computed from the reverse process of inserting a single solute molecule from a pure gas into its own pure liquid or subcooled liquid state, which is its self-solvation free energy (ΔG_{self}). This related to the vapor pressure P^X_{vap} of a liquid solute (X = liq) or of a subcooled liquid (X = subco) by[33]

$$P^X_{vap} = P^0 M_X \exp\left(\frac{\Delta G_{self}}{RT}\right) \quad (1)$$

where P^0 = 24.45 atm is the ideal gas pressure at 298 K at a density of 1 mol per liter and M_X is the molarity of the solute in its pure liquid or subcooled liquid state. The vapor pressure of a solid (P^{sol}_{vap}) can be calculated on the basis of eq 1 after correction using the melting temperature (T_m) and entropy of fusion (ΔS_{fus})[40] as follows:

$$P^{solid}_{vap} = P^{subco}_{vap} \exp\left\{\frac{\Delta S_{fus}}{R}\left(1 - \frac{T_m}{T}\right)\right\} \quad (2a)$$

When ΔS_{fus} is unknown, Yalkowsky[41] suggested a value of 13.5 cal/mol·K for rigid molecules at room temperature, so that

$$P^{solid}_{vap} = P^{subco}_{vap} \exp\{0.023(25 - T_m(^\circ C))\} \quad (2b)$$

The solubility of a solute in a solvent, S^X_{solv} (where the superscript has the same meaning as before, and the subscript solv designates either water or 1-octanol as the solvent) can be calculated from[32]

$$S^X_{solv} \equiv M^X_{solv} = \left(\frac{P^X_{vap}}{P^0}\right) \exp\left[-\frac{\Delta G_{solv}}{RT}\right] \quad (3)$$

where ΔG_{solv} is the solvation free energy in either water (ΔG_{wat}) or 1-octanol (ΔG_{oct}), M^X_{solv} is the solubility of the solute in the solvent in molarity units, and the superscript and subscript have the same meanings as before. However, to use eq 3 to calculate the solubility of a solid solute (S^{sol}_{solv}), the free energy of solvation also needs to be corrected with the solid state vapor pressure using one of eqs 2. For solutes in the liquid or subcooled state at room temperature, eq 3 can be simplified as follows

$$S^X_{solv} \equiv M^X_{solv} = M_X \exp\left[\frac{\Delta G_{self} - \Delta G_{solv}}{RT}\right] \quad (4)$$

The solubility of a room temperature solid solute (or crystal) can be thought of occurring in the three steps shown in Figure 1. The first step is to melt the solid at room temperature

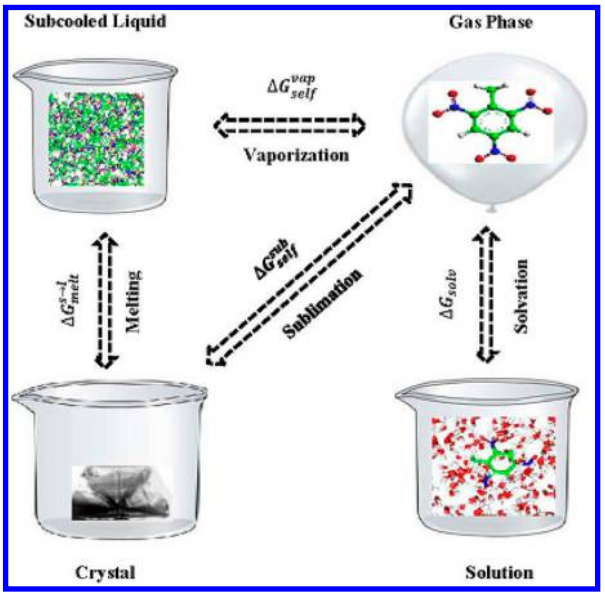

Figure 1. Model of solubility.

producing a melt below its melting temperature, that is, a subcooled liquid. Experimentally, cooling a liquid system below its freezing point temperature without crystallization can be realized by slow cooling in the absence of nucleation sites. In molecular simulation, this quenching process can be accomplished by starting at very low density and gradually compressing the system until it reaches the solid density at room temperature without solidification. The next step in computing the solvation free energy is to transfer a molecule from its subcooled liquid state to the gas phase, and this is related to the subcooled liquid vapor pressure. The third step is the solvation of the molecule in the solvent of interest. Thus, vapor pressure, solubility, and Henry's law constant at a subcooled state can be computed directly from molecular simulation results; however, the subcooled liquid-to-solid state corrections, as discussed above, are necessary.

The logarithms of octanol–water partition coefficients ($\log_{10} K_{OW}$) can be calculated from the solvation free energies in water (ΔG_{wat}) and octanol (ΔG_{oct}) using the following relation:[42−46]

$$\log_{10} K_{OW} = \frac{(\Delta G_{wat} - \Delta G_{oct})}{2.303RT} \quad (5)$$

dx.doi.org/10.1021/ct301129x | J. Chem. Theory Comput. 2013, 9, 2389−2397

where R is the universal gas constant and T is the temperature in degrees Kelvin. The logarithms of the air−water ($\log_{10} P_{AW}$) and air−octanol ($\log_{10} P_{AO}$) partition coefficients are calculated from

$$\log_{10} K_{AW} = -\frac{\Delta G_{wat}}{2.303RT} \text{ and } \log_{10} K_{AO} = -\frac{\Delta G_{oct}}{2.303RT} \quad (6)$$

The Henry's law constant (HLC) is calculated from

$$H^X_{wat} = \frac{P^X_{vap}}{S^X_{wat}} \quad (7)$$

B. Simulation Details. *i. Algorithm.* All simulations were carried out at room temperature and 1 atm pressure using the expanded ensemble (EE)[47−49] algorithm. Compared to other available methods,[50−53] the expanded ensemble algorithm has previously been found to be computationally efficient.[42,43] Also, the availability of built-in internal phase space convergence criteria and error tracking has made it an attractive choice for the calculation of solvation free energies. The details of the algorithm can be found elsewhere.[42,43,47,48,52,54]

ii. Force Field and Partial Atomic Charges. The CHARMM Generalized Force Field (CGenFF)[55] and Transferable Potentials for Phase Equilibria Simulations (TraPPE-UA)[56−59] force fields (FF) and their parameters were used for modeling both the ECs (with the exception of atomic charges) and the solvent 1-octanol. Previously, the TraPPE-UA model was found to predict hydration free energies of alkyl aromatics reasonably well.[60−62] Similar predictions of hydration free energies have been presented elsewhere with other force fields[63−69] and different sets of compounds, however, not for the nitroaromatic compounds considered here. TraPPE FF was not parametrized for nitroaromatic compounds studied here. United atom TraPPE parameters were used here for both the methyl group[57] and the aromatic ring,[58] and explicit hydrogen parameters were used for the nitro group.[58] TraPPE FF default charges for the atoms representing united atoms are zero; however, charges for nitro group atoms together with the charge of the carbon atom connected to the nitro group sum to zero, which maintains the neutrality of the compound and is true for any number of nitro groups connected to the aromatic ring. Rai and Siepmann[70] indicated that the default atomic charges are not usually transferrable to other molecules with different functionality in the presence of a resonance structure. A test set of solvation free energies in water was calculated using TraPPE default charges and summarized in Table ST10 of the Supporting Information (SI) that shows that the default charges lead to significant errors. Also, for the purpose of computing useful physicochemical properties, solvation free energies using CHELPG charges were calculated. Charge reassignment using quantum methods has been used previously with different force fields and led to improved hydration free energy predictions,[60,67,71−75] and this is also done here. The TIP3P[76] water model was used in all of the calculations of solvation free energies in water.[39] Initial molecular geometries were generated using ArgusLab 4.0.1[77] and then optimized in the gas phase using Gaussian 09[78] at the B3LYP/6-31G(d) level. The CHELPG[79] charges were then calculated using Gaussian 09 at the B3LYP/6-311G(d,p) level[80−83] and used with both force fields. ParamChem[84] charges were used to model the CGenFF 1-octanol model; however, the default charges were used with the TraPPE-UA 1-octanol model. The parameters for both CGenFF[55] and TraPPE-UA[56−59] force fields were collected from the literature; the CGenFF atom types and parameters were obtained using the ParamChem[84] webpage.

iii. Simulation Conditions. All simulations were carried out in the EE-NPT[47,48] (expanded ensemble isothermal−isobaric) ensemble with the temperature and pressure regulated by the Nose−Hoover[85,86] thermostat and barostat with relaxation times of 30 and 700 fs, respectively. All the van der Waals interactions were truncated at 12 Å, and long-range corrections added.[87] Thirty and 35 subensembles were used for the computations of the solvation free energies in 1-octanol and self-solvation free energies, respectively. An insertion parameter (λ_m) value was assigned to each of the subensembles using an index number (m) for the subensemble of interest and the total number of the subensembles (M) according to the scheme[49] $\lambda_m = (M - m)/(M - 1)$. The Lennard-Jones well depths of the solute atoms were scaled with the fourth power of λ_m, and the partial charges were scaled as the square of the insertion parameter.[48,49] Coulombic interactions were treated using the Ewald summation method,[88,89] and the Lorentz−Berthelot mixing rules[89] were used for all simulations.

The balancing factors in the EE method were optimized automatically using the Wang−Landau algorithm,[48,90,91] with the first 8.8 ns of the simulation times used to optimize the balancing factors during the solvation and self-solvation free energy computations using a scaling factor of 0.5 for the Wang−Landau iterations. In each simulation, a single solute molecule was inserted into 200 molecules either of 1-octanol (solvation) or of the same species as the solute (self-solvation). Solvation free energies in 1-octanol using the CGenFF and TraPPE-UA force fields were calculated with the multiple time step (long and short time steps of 2 and 0.5 fs, respectively) integration method of Tuckerman et al.,[92] and each simulation was run for 20 ns. The self-solvation free energies using TraPPE-UA FF were computed using the SHAKE constrained algorithm[87,89] with a time step of 1 fs to integrate the trajectories, and a complete self-solvation simulation was run for 20 ns.

For the room temperature solids (all ECs except 2-NT and 3-NT), simulations in the subcooled liquid states were carried out at room temperature and 1 atm pressure. The subcooled systems were prepared starting from a large volume that was gradually compressed to the solid densities at room temperature. Since experimental data are not available for the subcooled liquid densities of nitroaromatic compounds, the subcooled liquid systems were generated at solid densities assuming that the density difference will not exceed the average density fluctuations that occur during isothermal−isobaric simulations. Each volume compression was followed by a 100 to 200 fs isothermal−isobaric (NVT) simulation. Before collecting the simulation data, it was verified that all the convergence criteria[42,43] were satisfied (see Figures SF5−SF8 in the SI).

C. Critical Compilation and Comparison of Experimental Data. Experimental data for the physicochemical properties of ECs are sparse, and often there are considerable differences among the reported values from different investigators, as can be seen in the data in Tables ST2 and ST3, respectively, of the SI. There are no reported experimental solvation free energies for the ECs in 1-octanol, so these were calculated here from measured octanol−water partition coefficients[15,93−95] and solvation free energies in water[39] using eq 5. The accuracies of the reported solvation free

energies in water have been examined by us previously.[39] In Table ST4 of the SI, we have collected the ranges of experimental $\log_{10} K_{OW}$ data for the ECs and the recommended data we used for comparison with the calculation here. These data were chosen by comparing the data in the experimental database of EPIWEB 4.1,[93] those of Hansch et al.,[94] those of the LOGKOW[95] web databank, and the recommended values of Sangster.[15] The EPIWEB 4.1 database did not have the datum for log K_{OW} of 2,3-DNT and reports an estimated value of 2.18. The experimental datum of Verschueren[96] and adopted by Prak[97] was 2.0. Comparing with the recommended data for 2,4-DNT, 2,6-DNT, and 3,4-DNT, the value of Verschueren[96] was thought to be preferable and was chosen for 2,3-DNT. The data for 2,6-DNT in EPIWEB 4.1 was from a single source[98] and differs from the value recommended by Sangster.[15,95] Since the EPIWEB 4.1 log K_{OW} value was smaller compared to the other isomers of dinitrotoluene, the Sangster value was used here (Table ST4 of the SI). For a similar reason, the recommended value of Sangster[15,95] was chosen for 2,4,6-TNT (1.73).

Reported room temperature vapor pressures for the ECs are often extrapolated from high temperature experimental data using the Clausius−Clapeyron equation with fitted coefficients (for example, Table ST2 of the SI). The uncertainties in such reported values depend on the number of temperature data points and whether the temperature range is close to room temperature. We have collected data (Table ST5 of the SI) from different sources, compared them, and in some cases then used an arithmetic average of the values thought to be reliable. The details of the data sources are given in Table ST2 of the SI, and the data used for the comparison with the simulation results are summarized in Table ST5. The largest discrepancies (slightly more than a factor of 2) were found for the vapor pressures of 3-NT and 2,4,6-TNT, and the averages have standard deviations of ±0.29 and ±0.25 log units (for pressure in Pa), respectively. For the solid ECs, the measured subcooled liquid vapor pressures were collected (Table ST5 of the SI) from EPIWEB 4.1.[93] Data for the self-solvation free energies of the ECs have not been reported in the literature and were calculated here from the measured subcooled liquid vapor pressures using eq 1 and are compiled in Table ST6 of the SI.

The aqueous solubilities of the ECs reported in different sources (Table ST3 of the SI) vary widely. In some cases, the reported experimental room-temperature aqueous solubilities of the ECs were in fact calculated from a group contribution method, estimated by extrapolation, or were measured at a slightly different temperature, usually in the range of 20 to 30 °C.[99] These data were compared with the experimental database in EPIWEB 4.1[93] and the data reported by Mackay et al.,[99] whenever possible. If several data were found to be in reasonably close agreement, an average value was used. There are no reported solubilities for the ECs in 1-octanol found in the literature. The values we use here for comparison were calculated from the measured vapor pressures and solvation free energies in 1-octanol using eq 3. The subcooled liquid aqueous and 1-octanol solubilities of the ECs also were not found in the literature; they were calculated here from the measured vapor pressures of the subcooled liquid and the solvation free energies in water and 1-octanol using eq 3 and are compiled in Table ST7 of the SI.

The air−water and air−octanol partition coefficients were calculated from the solvation free energies in water and in 1-octanol using eq 6 (Table ST8 of the SI). The measured Henry's law constant data were collected (Table ST9 of the SI) from EPIWEB 4.1;[93] however, no experimental data were found for 2,3-DNT and 3,4-DNT, so that comparisons were made only for those solutes with available experimental data.

III. RESULTS

Solvation free energies in 1-octanol were calculated using the TraPPE-UA/CHELPG and CGenFF/CHELPG models for the ECs and summarized in Table 1. However, since the predictions using the TraPPE-UA/CHELPG model were found to be superior to those of the CGenFF/CHELPG model, most calculations were done only with the former. Self-solvation free energies of ECs were calculated only using TraPPE-UA/CHELPG models. The solvation free energies in water (Table ST10 of the SI) for the calculation of the partition coefficients are from our previous work[39] using the same force fields and charges. Table 2 summarizes the average unsigned (AUE) and root-mean-square errors (RMSE) over all compounds of the computed solvation free energies in 1-

Table 1. Solvation Free Energy of ECs in 1-Octanol (ΔG_{oct}) in kcal/mol

NACs	experiment	TraPPE	CGenFF
2-NT	−6.82	−6.13 ± 0.19	−6.82 ± 0.16
3-NT	−6.79	−5.77 ± 0.20	−6.80 ± 0.20
4-NT	−7.39	−6.11 ± 0.12	−7.54 ± 0.23
2,3-DNT	−9.10	−8.05 ± 0.28	−10.34 ± 0.30
2,4-DNT	−9.47	−9.40 ± 0.35	−10.30 ± 0.28
2,6-DNT	−8.95	−8.47 ± 0.30	−10.19 ± 0.24
3,4-DNT	−9.59	−8.83 ± 0.31	−11.14 ± 0.44
2,4,6-TNT	−10.79	−11.32 ± 0.32	−12.77 ± 0.41
1,3,5-TNB	−11.10	−11.22 ± 0.31	−14.08 ± 0.43
AUE (kcal/mol)		0.67	1.11
RMSE (kcal/mol)		0.77	1.45

Table 2. Summary of All Calculations Presented Here Using TraPPE-UA/CHELPG Force Field[a]

physicochemical property	AUE	RMSE	Table[b,c]
ΔG_{oct} (kcal/mol)	0.67 (1.11)	0.77 (1.45)	1
ΔG_{self}^{liq} (kcal/mol)	0.44	0.44	ST11
ΔG_{self}^{subco} (kcal/mol)	0.52	0.83	ST11
$\log_{10} P_{vap}^{subco}$ (pressure in Pa)	0.38	0.61	ST12
$\log_{10} P_{vap}^{liq}$ (pressure in Pa)	0.35	0.35	ST12
$\log_{10} P_{vap}^{liq/sol}$ (pressure in Pa)	0.61	0.78	ST12
$\log_{10} S_{wat}^{subco}$ (S in mol/L)	0.71	0.75	ST13
$\log_{10} S_{wat}^{liq/sol}$ (S in mol/L)	0.26	0.29	ST13
$\log_{10} S_{oct}^{subco}$ (S in mol/L)	0.47	0.60	ST13
$\log_{10} S_{oct}^{liq/sol}$ (S in mol/L)	0.37	0.43	ST13
$\log_{10} K_{OW}$	0.45 (0.55) [0.13]	0.51 (0.74) [0.16]	ST14
$\log_{10} K_{AW}$	0.44 (0.45) [1.09]	0.51 (0.49) [1.35]	ST15
$\log_{10} K_{AO}$	0.49 (0.81)	0.57 (1.06)	ST15
$\log_{10} H_{wat}^{sol/liq}$ (H in Pa-m^3/mol)	0.73	0.77	ST16

[a]The values in parentheses and square brackets are from the CGenFF/CHELPG force field and Abraham's method (see section III of the SI for details), respectively. [b]Tables in the Supporting Information (SI) list component-by-component results. [c]ST means the Table in the Supporting Information.

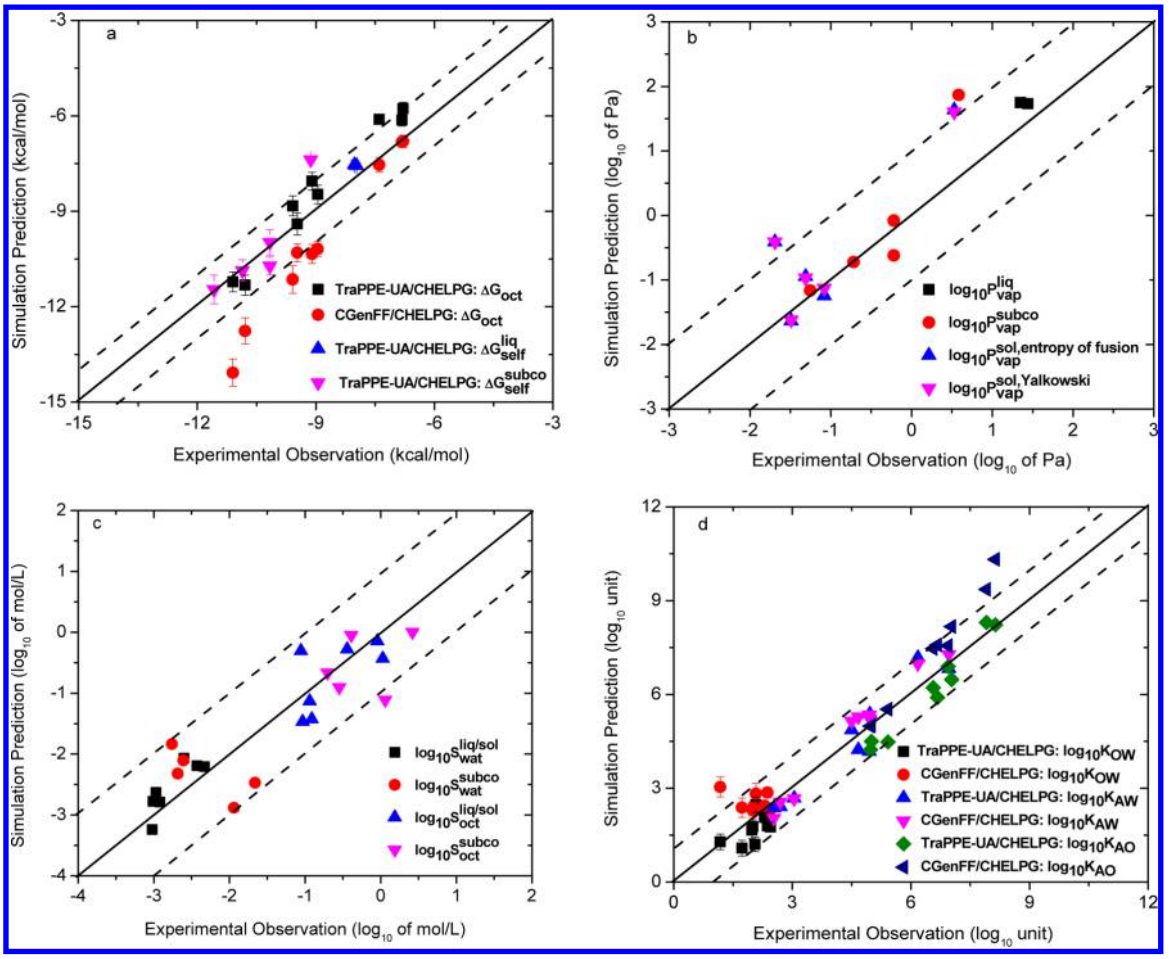

Figure 2. Comparison of predicted (from simulation) and measured values of (a) ΔG_{oct} and ΔG_{self}, (b) vapor pressures (liquid, solid, and subcooled), (c) solubilities (liquid, solid, and subcooled), and (d) partition coefficients (K_{OW}, K_{AW}, K_{AO}) for ECs. The solid lines represent perfect correlation with experimental data, and the dashed lines indicate (a) ± 1 kcal/mol, (b) ± 1 $\log_{10}$ of Pa, (c) ± 1 $\log_{10}$ of mol/L, and (d) ± 1 $\log_{10}$ unit, and most predictions are within ±1 unit of the respective scales.

octanol, self-solvation free energies, vapor pressures, solubilities (in water and 1-octanol), and the Henry's law constants for both liquid and subcooled liquid components and also the partition coefficients (air−water, air−octanol, octanol−water) using the TraPPE-UA/CHELPG model. Some of these properties were also computed using CGenFF/CHELPG models, and these are shown in parentheses in the table. Data for each component used in the calculations of the statistics can be found in Table 1 and Tables ST10−ST16 of the SI.

The use of the TraPPE-UA/CHELPG model in simulation reproduced experimental solvation free energies in 1-octanol with an average unsigned error (AUE) of 0.67 kcal/mol and root-mean-square error (RMSE) of 0.77 kcal/mol, which was better than the CGenFF/CHELPG model, which led to an AUE of 1.11 kcal/mol and RMSE of 1.45 kcal/mol (Table 1). Also the deviations from experimental data using the CGenFF/CHELPG model increases with the number of nitro groups and was largest for 1,3,5-TNB. The AUE of the solvation free energies of nitroaromatic compounds in water using TraPPE-UA/CHELPG was 0.61 kcal/mol. It is to be noted that experimental solvation free energies in 1-octanol were calculated from the measured hydration free energies and $\log_{10} K_{OW}$ data. Since measured $\log_{10} K_{OW}$ values for most of the nitroaromatics studied here vary between ∼0.15 and 0.5 log units (Table ST4 of the SI) and there are also uncertainties in the experimental hydration free energies, this level of prediction is quite reasonable. If we would have used measured hydration free energies instead of the simulation results, we could have obtained ∼0.21 to 0.68 kcal/mol differences in magnitude of the 1-octanol solvation free energies due to 0.15 to 0.5 log unit variations in $\log_{10} K_{OW}$ values.

Table ST11 of the SI compares the self-solvation free energies of the ECs calculated using the TraPPE-UA/CHELPG model with experimental data. For the liquid ECs, the TraPPE-UA/CHELPG model used in simulation reproduces the experimental data with both an AUE and RMSE of 0.44 kcal/mol. The errors are greater for the solid ECs, reproducing the experimental self-solvation free energies with an AUE 0.52 kcal/mol and RMSE 0.83 kcal/mol. The subcooled liquid vapor pressures of ECs calculated from the subcooled self-solvation free energies of Table ST11 of the SI are presented in Table ST12 of the SI. The TraPPE-UA/CHELPG force field reproduces the experimental subcooled liquid vapor pressures with an AUE of 0.38 log unit (in Pa) and RMSE of 0.61 log unit, with the largest deviation from experiment for 4-NT.

Table ST12 of the SI also presents the data for liquid and solid room temperature vapor pressures of the ECs calculated using the corrections for subcooled-to-solid state transition, eqs 2a and 2b. For the liquid ECs, TraPPE-UA/CHELPG models

predict vapor pressures with an AUE of 0.35 $\log_{10}$ unit (in Pa); for the room temperature solid ECs, the vapor pressures calculated using either of eqs 2 are less precise. The model of Yalkowsky predicts solid state vapor pressure with an AUE of 0.58 $\log_{10}$ unit (in Pa), slightly better than using the entropy of fusion and melting temperature for which the AUE is 0.61 $\log_{10}$ unit (in Pa).

For the partition coefficients $\log_{10} K_{OW}$ (Table ST14(a) of the SI), $\log_{10} K_{AW}$ (Table ST15 of the SI), and $\log_{10} K_{AO}$ (Table ST15 of the SI), the predictions of the TraPPE-UA/CHELPG model are more accurate with AUEs of 0.45, 0.44, and 0.49, respectively, in $\log_{10}$ units compared to the CGenFF/CHELPG model predictions for which the AUEs are 0.55, 0.45, and 0.81 log units, as shown in Table 2. The HLCs (Table ST16 of the SI) calculated from the vapor pressures (Table ST12 of the SI) and solubilities (Table ST13 of the SI) of the sparingly soluble ECs have an AUE of 0.73 $\log_{10}$ unit (in Pa-m^3/mol). The predicted HLCs of the subcooled ECs are also presented in that table, but there are no experimental data with which to compare.

Figure 2 shows the correspondence between the simulation predictions and experimental data. Most predictions are within ±1 unit of their respective scales used in Figure 2a−d. The outliers in Figure 2a are due to the solvation free energies in 1-octanol using CGenFF/CHELPG models, and this scatter is also reflected in Figure 2d as outliers in $\log_{10} K_{AW}$ calculated using the same models. The solid state vapor pressure corrections lead to scatter for the two data points in Figure 2b, and so that for ECs the solid state correction of eqs 2 may not be adequate since the melting point temperatures are quite far from the room temperature. The scatter in Figure 2c is largely from the subcooled liquid solubilities in water and 1-octanol with only one point deviating from experiment by 1 $\log_{10}$ unit (in mol/L).

IV. DISCUSSION

Considering the uncertainties in measured $\log_{10} K_{OW}$ data (0.15 to 0.5 log units in Table ST4 of the SI) of nitroaromatic compounds, our predictions with an AUE of 0.45 log unit are quite reasonable and justify the suitability of using CHELPG charges with the TraPPE force field. Recently, Jämbeck et al.[48] found that for a test set of multifunctional compounds, including some nitrogen-containing compounds, the best predictions for the free energies of hydration had an RMS error of 2.33 kcal/mol using the restrained-ESP (RESP) method together with effectively polarized charges. Their predictions of $\log_{10} K_{OW}$ from the solvation free energies in water and 1-octanol were computed using polarized charges obtained from the self-consistent reaction field method (SCRF) using water and 1-octanol solvents independently; they found that the root-mean-square errors (RMSE) of their predictions (1.3 log unit) differed by only 0.1 log unit compared to that of using gas phase RESP charges (1.4 log unit) in both the water and octanol phases. Therefore, the use of gas phase charges is not unreasonable. It is to be noted that not only the partial atomic charges but also the van der Waals forces play a significant role in the solvation in 1-octanol due to its limited polarity.[100]

The problem with the parametrization of multifunctional nitroaromatic compounds can be partly attributed to the limitation of resolving steric effects involved. For substituted aromatics, the spatial positions of the functional groups are also important as suggested by Fennell and Dill.[101] For multi-substituted nitroaromatics, the relative position of the nitro groups to one another and to the methyl group is also important in determining the solvent accessible surface area or volume and surface curvature. At least a qualitative understanding of such steric effects can be gained looking at the CHELPG charges computed here. The distribution of the charges on the nitro group nitrogen and oxygen atoms vary depending on the relative position and orientation of the methy group and nitro groups. Also, the charges on the aromatic carbons vary with the location and relative position of the substituents. Although we can get some idea about the steric interactions and the effects of orientation of atoms in the functional groups looking at the CHELPG charges, a useful description of such effects is out of the scope of the current manuscript.

Most of the reported experimental solid state vapor pressures are extrapolated values, as can be seen from Table ST2 of the SI. Given the extent of uncertainties in the experimental determination of vapor pressures of the subcooled liquid ECs, the results obtained from the TraPPE-UA/CHELPG models are considered to be quite good.

Winget et al.[33] reported the vapor pressure of 2-NT (in natural log of Torr and here converted to $\log_{10}$ in Pa) calculated using different versions of Minnesota solvation models.[102] Table ST18 of the SI shows a comparison of the measured value, the prediction from our simulation using the TraPPE-UA/CHELPG force field, and the predictions of the different solvation models. The TraPPE-UA/CHELPG predictions are superior to many of the solvation model results and comparable to the results of the MM3/SM5.0R and MM2/SM5.0R solvation models. Table ST19 of the SI shows the comparison of the liquid and solid vapor pressures computed here and predicted from the Antoine, Grain, and modified Grain methods using EPIWEB 4.1.[93] For the liquid ECs, the TraPPE-UA/CHELPG model predictions are better than the mean vapor pressures estimated from Antoine and Grain methods. Also, the solid state vapor pressures computed using the TraPPE-UA/CHELPG model with the corrections of eq 2 are in reasonable agreement with the predictions of Antoine, Grain, and modified Grain methods. The largest deviation from experimental data of the TraPPE-UA/CHELPG prediction is for 4-NT, and both simulation and EPIWEB 4.1 predictions are poor for 3,4-DNT.

Using the Minnesota solvation models, Thompson et al.[32] calculated solubilities of 2-NT and 4-NT (Table S-XII of the SI of ref 32), which are compared with experimental and our simulation results in Table ST20 of the SI. The TraPPE-UA/CHELPG model predictions of the solubility of 2-NT are better than the HF/SM5.42R and AM1/SM5.42R solvation models and comparable to the B3LYP/SM5.42R model predictions. For 4-NT, the prediction from the B3LYP/SM5.42R is the most accurate followed by the TraPPE-UA/CHELPG prediction. However, it is to be noted that Thompson et al.[32] used measured room temperature vapor pressures with the solvation free energies calculated from the various solvation models to calculate the solubilities, while in our calculations the vapor pressures were obtained from the self-solvation free energies (for the solid 4-NT, an additional correction was made for the solid state vapor pressure using eqs 2) so that no experimental data were used. For the compounds compared here, the TraPPE-UA/CHELPG model and EE simulation without the use of any experimental data are quite good in reproducing the measured solubilities of the ECs. Also,

the differences in accuracy of the various solvation models raise the issue of the user knowing *a priori* which would be best for a specific property.

The logarithms of K_{AW} obtained from simulations are compared with the calculated values using Abraham descriptors (the details of that calculation method can found in the SI: eq SI_1 and Tables ST17 and ST21), and it is found that both TraPPE-UA/CHELPG and CGenFF/CHELPG models led to $\log_{10} K_{AW}$ predictions that are more accurate than the Abraham method. For $\log_{10} K_{OW}$ predictions, the Abraham method led to more accurate predictions (values in the square brackets in Table 2 and in Table ST22 of the SI) than both the TraPPE-UA/CHELPG and CGenFF/CHELPG models. Chen and Siepmann[103] found that for alcohol solutes the solvation free energies in dry 1-octanol are approximately 0.24 kcal/mol more negative than that of wet 1-octanol, which leads to overestimates of the $\log_{10} K_{AO}$ and $\log_{10} K_{OW}$ predictions by approximately 0.18 log units. The local solvation structures of alcohol solutes are thought to be responsible for this. However, recently it has been reported[104] that for *n*-alkanes $\log_{10} K_{OW}$ predictions using wet 1-octanol are underestimated by 0.2−0.4 log units compared to using dry 1-octanol. Without further study, the effect of dry and wet 1-octanol on the solvation of nitroaromatic compounds cannot be predicted.

In Table ST23 of the SI, we have collected the HLC data from experimental results, calculated from experimental vapor pressures and solubilities, and predicted from group contribution and bond methods as implemented in EPIWEB4.1.[93] This table also shows the statistics of the HLCs calculated using the different methods compared to experimental results. The accuracy of the predictions for the HLCs is in the order of the bond method > group method > TraPPE-UA/CHELPG (EE simulation). While the empirical methods, especially the bond method, lead to more accurate HLC predictions, the TraPPE-UA FF simulation results are in reasonable agreement with the experimental data and do not require any experimental data in the calculations.

V. CONCLUSIONS

We have presented here a reliable method for predicting a range of thermophysical properties from molecular simulation that is completely predictive and requires only the connectivity of the atoms. No experimental data are used. The results demonstrate that the protocol relating the thermodynamic properties to the simulations is reliable and reasonably accurate with an appropriate choice of force field and atomic charges. One of the advantages of the method is the ability to predict the vapor pressure of liquid and subcooled liquid (solid at room temperature) ECs in the pressure range of 10^{-1} to 10^{-6} mm Hg where measurements can be difficult; for subcooled liquids, direct measurement techniques are nonexistent. Another advantage of the method presented here is that it can also be used to predict the solubilities of solutes in 1-octanol as was done here, but in other solvents as well. In principle, the method used here can be applied to any solvent−solute pair.

The reliability of the method has been examined here by predicting the three most important partition coefficients (octanol−water, air−water, and air−octanol) with average unsigned error of less than 0.5 log units. The method can also be used to predict the partitioning solutes in different air−solvent and solvent−solvent pairs, for example, the hexane−water, toluene−water, and chloroform−water partition coefficients that are used for environmental characterization. The method can also be used for the prediction of Henry's law constants of sparingly soluble compounds and subcooled liquids, an important component in many environmental models, but for which experimental data are scarce.

The most important feature of this method, in contrast to empirical and semiempirical methods, is that it is completely predictive, does not rely on any experimental data, and uses only the atomic connectivity. Therefore, the method can be used for any molecule, including those not yet synthesized. So it has value for predicting thermophysical properties of materials for which experimental measurement is difficult, for screening the pharmacological behavior of novel drugs, and predicting the likely environmental impact of new chemicals, energetic materials, or other hazardous compounds.

■ ASSOCIATED CONTENT

Ⓢ Supporting Information

Figures SF1−SF8: molecular structures of ECs (SF1), fitting of solubility data (SF2−SF4), and the convergence tests of EE simulations (SF5−SF8) in the self-solvation free energy computations. Tables ST1−ST23: molecular and thermophysical properties of ECs (ST1), compilations of experimental physicochemical properties data (ST2−ST9), comparison of simulation results with experimental data (ST10−ST16), data calculated using Abraham method (ST17), and comparison of simulation data with available data from other methods (ST18−ST23). This material is available free of charge via the Internet at http://pubs.acs.org.

■ AUTHOR INFORMATION

Corresponding Author

*Phone: 302-831-2945. Fax: 302-831-8201. E-mail: sandler@udel.edu.

Notes

The authors declare no competing financial interest.

■ ACKNOWLEDGMENTS

This work has been supported by National Science Foundation (NSF) grant GOALI-0853685 and the Strategic Environmental Research and Development Program (SERDP) grant ER-1734. This work used the Extreme Science and Engineering Discovery Environment (XSEDE), which is supported by National Science Foundation grant number OCI-1053575.

■ REFERENCES

(1) Shiu, W. Y.; Mackay, D. *J. Phys. Chem. Ref. Data* **1986**, *15*, 911−929.
(2) Burkhard, L. P.; Armstrong, D. E.; Andren, A. W. *Environ. Sci. Technol.* **1985**, *19*, 590−596.
(3) Dunnivant, F. M.; Elzerman, A. W. *Chemosphere* **1988**, *17*, 525−541.
(4) Doskey, P. V.; Andren, A. W. *Environ. Sci. Technol.* **1981**, *15*, 705−711.
(5) Junge, C. E. In *Fate of Pollutants in the Air and Water Environments: Part 1. Mechanisms of Interactions between Environments and Mathematical Modeling and the Physical Fate of Pollutants*; Suffet, I. H., Ed.; Wiley: NewYork, 1977; pp 7−25.
(6) Pankow, J. F. *Atmos. Environ.* **1987**, *21*, 2275−2283.
(7) Bidleman, T. F.; Falconer, R. L.; Harner, T. In *Gas and Particle Phase Measurements of Atmospheric Organic Compounds*; Lane, D. A., Ed.; Gordon and Breach: Amsterdam, 1999; pp 39−71.
(8) Lei, Y. D.; Chankalal, R.; Chan, A.; Wania, F. *J. Chem. Eng. Data* **2002**, *47*, 801−806.
(9) Pankow, J. F. *Atmos. Environ.* **1994**, *28*, 189−193.

(10) Pankow, J. F. *Atmos. Environ.* **1994**, *28*, 185−188.
(11) Haftka, J. J. H.; Parsons, J. R.; Govers, H. a J. *J. Chromatogr., A* **2006**, *1135*, 91−100.
(12) Hinckley, D. A.; Bidleman, T. F.; Foreman, W. T.; Tuschall, J. R. *J. Chem. Eng. Data* **1990**, *35*, 232−237.
(13) Chickos, J. S.; Hanshaw, W. *J. Chem. Eng. Data* **2004**, *49*, 620−630.
(14) *Risk Assessment of Chemicals: An Introduction*, 2nd ed.; van Leeuwen, C. J., Vermeire, T. G., Eds.; Springer: New York, 2007; p 688.
(15) Sangster, J. *Octanol-Water Partition Coefficients: Fundamentals and Physical Chemistry*; John Wiley & Son Ltd: New York, 1997.
(16) Connel, D. W. *Bioaccumulation of Xenobiotic Compounds*; CRC Press Inc.: Boca Raton, FL, 1990; p 213.
(17) Briggs, G. G. *J. Agric. Food Chem.* **1981**, *29*, 1050−1059.
(18) Connell, D. W.; Braddock, R. D.; Mani, S. V. *Sci. Total Environ.* **1993**, *134*, 1383−1396.
(19) Lian, G.; Chen, L.; Han, L. *J. Pharm. Sci.* **2008**, *97*, 584−598.
(20) Hansch, C.; Kim, D.; Leo, A. J.; Novellino, E.; Silipo, C.; Vittoria, A. *Crit. Rev. Toxicol.* **1989**, *19*, 185−226.
(21) Hansch, T. F. *J. Am. Chem. Soc.* **1964**, *86*, 1616−1626.
(22) Hansch, C.; Leo, A.; Hoekman, D. *Exploring QSAR - Hydrophobic, Electronic, and Steric Constants*; American Chemical Society: Washington, DC, 1995.
(23) Finizio, A.; Mackay, D.; Bidleman, T.; Harner, T. *Atmos. Environ.* **1997**, *31*, 2289−2296.
(24) Shoeib, M.; Harner, T. *Environ. Toxicol. Chem.* **2002**, *21*, 984−990.
(25) Kelly, B. C.; Ikonomou, M. G.; Blair, J. D.; Morin, A. E.; Gobas, F. A. P. C. *Science* **2007**, *317*, 236−239.
(26) Harner, T.; Bidleman, T. F. *J. Chem. Eng. Data* **1996**, *41*, 895−899.
(27) Harner, T.; Mackay, D. *Environ. Sci. Technol.* **1995**, *29*, 1599−606.
(28) *Handbook of Property Estimation Methods for Chemicals: Environmental Health Sciences*; Mackay, D., Boethling, R. S., Eds.; CRC Press: Boca Raton, FL, 2000; p 504.
(29) Harner, T.; Bidleman, T. F. *Environ. Sci. Technol.* **1998**, *32*, 1494−1502.
(30) Debolt, S. E.; Kollman, P. A. *J. Am. Chem. Soc.* **1995**, *117*, 5316−5340.
(31) Giesen, D. J.; Hawkins, G. D.; Liotard, D. A.; Cramer, C. J.; Truhlar, D. G. *Theor. Chem. Acc.* **1997**, *98*, 85−109.
(32) Thompson, J. D.; Cramer, C. J.; Truhlar, D. G. *J. Chem. Phys.* **2003**, *119*, 1661−1670.
(33) Winget, P.; Hawkins, G. D.; Cramer, C. J.; Truhlar, D. G. *J. Chem. Phys. B* **2000**, *104*, 4726−4734.
(34) Chuang, Y.-Y.; Cramer, C. J.; Truhlar, D. G. *Int. J. Quantum Chem.* **1998**, *70*, 887−896.
(35) Chuang, Y.-Y.; Radhakrishnan, M. L.; Fast, P. L.; Cramer, C. J.; Truhlar, D. G. *J. Phys. Chem. A* **1999**, *103*, 4893−4909.
(36) Cramer, C. J.; Truhlar, D. G. In *Free Energy Calculations in Rational Drug Design*; Reddy, M. R., Erion, M. D., Eds.; Kluwer Academic/Plenum: New York, 2001; pp 63−95.
(37) Abraham, M. H. *Chem. Soc. Rev.* **1992**, *096*, 73−83.
(38) Katritzky, A. R.; Oliferenko, A. A.; Oliferenko, P. V.; Petrukhin, R.; Tatham, D. B. *J. Chem. Inf. Comput. Sci.* **2003**, *43*, 1794−1805.
(39) Ahmed, A.; Sandler, S. I. Hydration Free Energies of Multifunctional Nitroaromatic Compounds (to be submitted).
(40) Sandler, S. I. *Chemical, Biochemical, and Engineering Thermodynamics*, 4th ed.; Wiley: New York, 2006; p 960.
(41) Yalkowsky, S. H. *Ind. Eng. Chem. Fundam.* **1979**, *18*, 108−111.
(42) Yang, L.; Ahmed, A.; Sandler, S. I. *J. Comput. Chem.* **2013**, *34*, 284−293.
(43) Ahmed, A.; Sandler, S. I. *J. Chem. Phys.* **2012**, *136*, 154505.
(44) Jorgensen, L. *Acc. Chem. Res.* **1989**, 184−189.
(45) Jorgensen, W. L.; Briggs, J. M.; Contreras, M. L. *J. Phys. Chem.* **1990**, *94*, 1683−1686.
(46) Essex, J. W.; Reynolds, C. a.; Richards, W. G. *J . Chem. Soc., Chem. Commun.* **1989**, 1152−1154.
(47) Lyubartsev, A. P.; Førrisdahl, O. K.; Laaksonen, A. *J. Chem. Phys.* **1998**, *108*, 227−233.
(48) Jämbeck, J. P. M.; Mocci, F.; Lyubartsev, A. P.; Laaksonen, A. *J. Comput. Chem.* **2013**, *34*, 187−97.
(49) Lyubartsev, A. P.; Laaksonen, A. *Comput. Phys. Commun.* **2000**, *128*, 565−589.
(50) Chipot, C.; Pohorille, A. *Free Energy Calculations: Theory and Applications in Chemistry and Biology*; Springer: Berlin, 2007.
(51) Bennett, C. H. *J. Comput. Phys.* **1976**, *22*, 245−268.
(52) Lyubartsev, A. P.; Martsinovski, A. A.; Shevkunov, S. V.; Vorontsov-Velyaminov, P. N. *J. Chem. Phys.* **1992**, *96*, 1776−1783.
(53) Kirkwood, J. G. *J. Chem. Phys.* **1935**, *3*, 300−313.
(54) Lyubartsev, A. P.; Laaksonen, A.; Vorontsov-Velyaminov, P. N. *Mol. Phys.* **1994**, *82*, 455−471.
(55) Vanommeslaeghe, K.; Hatcher, E.; Acharya, C.; Kundu, S.; Zhong, S.; Shim, J.; Darian, E.; Guvench, O.; Lopes, P.; Vorobyov, I.; MacKerell, A. D., Jr. *J. Comput. Chem.* **2010**, *31*, 671−690.
(56) Martin, M. G.; Siepmann, J. I. *J. Phys. Chem. B* **1998**, *102*, 2569−2577.
(57) Wick, C. D.; Martin, M. G.; Siepmann, J. I. *J. Phys. Chem. B* **2000**, *104*, 8008−8016.
(58) Wick, C. D.; Stubbs, J. M.; Rai, N.; Siepmann, J. I. *J. Phys. Chem. B* **2005**, *109*, 18974−18982.
(59) Martin, M. G.; Siepmann, J. I. *J. Phys. Chem. B* **1999**, *103*, 4508−4517.
(60) Garrido, N. M.; Jorge, M.; Queimada, A. J.; Gomes, J. R. B.; Economou, I. G.; Macedo, E. A. *Phys. Chem. Chem. Phys.* **2011**, *13*, 17384−94.
(61) Garrido, N. M.; Queimada, A. J.; Jorge, M.; Macedo, E. a.; Economou, I. G. *J. Chem. Theory Comput.* **2009**, *5*, 2436−2446.
(62) Garrido, N. M.; Queimada, J.; Jorge, M.; Macedo, A. *AIChE J.* **2012**, *58*, 1929−1938.
(63) Kollman, P. *Chem. Rev.* **1993**, *93*, 2395−2417.
(64) Jorgensen, W. L.; Thomas, L. L. *J. Chem. Theory Comput.* **2009**, *4*, 869−876.
(65) Beveridge, D. L.; DiCapua, F. M. *Annu. Rev. Biophys. Biophys. Chem.* **1989**, *18*, 431−92.
(66) Gilson, M. K.; Zhou, H.-X. *Annu. Rev. Biophys. Biomol. Struct.* **2007**, *36*, 21−42.
(67) Mobley, D. L.; Bayly, C. I.; Cooper, M. D.; Shirts, M. R.; Dill, K. A. *J. Chem. Theory Comput.* **2009**, *5*, 350−358.
(68) Lewin, J.; Rai, N.; Maerzke, K.; Bhatt, D.; Siepmann, J.; Maiti, A.; Fried, L. In *Energetic Materials*; CRC Press: Boca Raton, FL, 2010; pp 63−76.
(69) Sokkalingam, N.; Potoff, J. J.; Boddu, V. M.; Maloney, S. W. In *Proceedings of the Army Science Conference (26th)*, Orlando, Florida, December 1−4, 2008; Assistant Secretary of the Army (Acquisition Logistics and Technology): Washington DC, 2008; p 7.
(70) Rai, N.; Siepmann, J. I. *J. Phys. Chem. B* **2007**, *111*, 10790−10799.
(71) Shivakumar, D.; Williams, J.; Wu, Y.; Damm, W.; Shelley, J.; Sherman, W. *J. Chem. Theory Comput.* **2010**, *6*, 1509−1519.
(72) Shivakumar, D.; Deng, Y.; Roux, B. *J. Chem. Theory Comput.* **2009**, *5*, 919−930.
(73) Mobley, D. L.; Dumont, E.; Chodera, J. D.; Dill, K. A. *J. Phys. Chem. B* **2007**, *111*, 2242−2254.
(74) Paluch, A. S.; Shah, J. K.; Maginn, E. J. *J. Chem. Theory Comput.* **2011**, *7*, 1394−1403.
(75) Jakalian, A.; Jack, D. B.; Bayly, C. I. *J. Comput. Chem.* **2002**, *23*, 1623−1641.
(76) Jorgensen, W. L.; Chandrasekhar, J.; Madura, J. D.; Impey, R. W.; Klein, M. L. *J. Chem. Phys.* **1983**, *79*, 926−935.
(77) Thompson, M. A. *ArgusLab 4.0.1*. http://www.arguslab.com/arguslab.com/ArgusLab.html.
(78) Frisch, M. J.; Trucks, G. W.; Schlegel, H. B.; Scuseria, G. E.; Robb, M. A.; Cheeseman, J. R.; Scalmani, G.; Barone, V.; Mennucci, B.; Petersson, G. A.; Nakatsuji, H.; Caricato, M.; Li, X.; Hratchian, H.

P.; Izmaylov, A. F.; Bloino, J.; Zheng, G.; Sonnenberg, J. L.; Hada, M.; Ehara, M.; Toyota, K.; Fukuda, R.; Hasegawa, J.; Ishida, M.; Nakajima, T.; Honda, Y.; Kitao, O.; Nakai, H.; Vreven, T.; Montgomery, J. A., Jr.; Peralta, J. E.; Ogliaro, F.; Bearpark, M.; Heyd, J. J.; Brothers, E.; Kudin, K. N.; Staroverov, V. N.; Kobayashi, R.; Normand, J.; Raghavachari, K.; Rendell, A.; Burant, J. C.; Iyengar, S. S.; Tomasi, J.; Cossi, M.; Rega, N.; Millam, J. M.; Klene, M.; Knox, J. E.; Cross, J. B.; Bakken, V.; Adamo, C.; Jaramillo, J.; Gomperts, R.; Stratmann, R. E.; Yazyev, O.; Austin, A. J.; Cammi, R.; Pomelli, C.; Ochterski, J. W.; Martin, R. L.; Morokuma, K.; Zakrzewski, V. G.; Voth, G. A.; Salvador, P.; Dannenberg, J. J.; Dapprich, S.; Daniels, A. D.; Farkas, O.; Foresman, J. B.; Ortiz, J. V; Cioslowski, J.; Fox, D. J. *Gaussian 09 User's Reference*; Gaussian, Inc.: Wallingford, CT, 2010.

(79) Breneman, C. M.; Wiberg, K. B. *J. Comput. Chem.* **1990**, *11*, 361−373.

(80) Becke, A. D. *J. Chem. Phys.* **1993**, *98*, 5648−5652.

(81) Lee, C.; Yang, W.; Parr, R. G. *Phys. Rev. B* **1988**, *37*, 785−789.

(82) Petersson, G. A.; Bennett, A.; Tensfeldt, T. G.; Al-Laham, M. A.; Shirley, W. A.; Mantzaris, J. *J. Chem. Phys.* **1988**, *89*, 2193−2218.

(83) Petersson, G. A.; Al-Laham, M. A. *J. Chem. Phys.* **1991**, *94*, 6081−6090.

(84) ParamChem. https://www.paramchem.org/AtomTyping/ (accessed May 04, 2012).

(85) Nosé, S. *J. Chem. Phys.* **1984**, *81*, 511−519.

(86) Hoover, W. G. *Phys. Rev. A* **1985**, *31*, 1695−1697.

(87) Sadus, R. J. *Molecular Simulation of Fluids: Theory, Algorithms, and Object-Orientation*; Elsevier: Amsterdam, 1999.

(88) Ewald, P. P. *Ann. der Phys.* **1921**, *369*, 253−287.

(89) Allen, M. P.; Tildesley, D. J. *Computer Simulation of Liquids*; Oxford University Press: New York, 1989.

(90) Wang, F.; Landau, D. P. *Phys. Rev. Lett.* **2001**, *86*, 2050−2053.

(91) Aberg, K. M.; Lyubartsev, A. P.; Jacobsson, S. P.; Laaksonen, A. *J. Chem. Phys.* **2004**, *120*, 3770−3776.

(92) Tuckerman, M.; Berne, B. J.; Martyna, G. J. *J. Chem. Phys.* **1992**, *97*, 1990.

(93) *EPIWEB 4.1*, v 4.10 (Estimation Programs Interface Suite for Microsoft Windows); U.S. EPA: Washington, DC, 2011.

(94) Hansch, C.; Leo, A. *Exploring QSAR: Vol. 1: Fundamentals and Applications in Chemistry and Biology*; Heller, S. R., Ed.; American Chemical Society: Washington, DC, 1995; p 584.

(95) Sangster Research Laboratories LOGKOW. http://logkow.cisti.nrc.ca/logkow/index.jsp (accessed Oct 3, 2012).

(96) Verschueren, K. *Handbook of Environmental Data on Organic Chemicals*, 4th ed.; John Wiley & Sons: New York, 2001.

(97) Prak, D. J. L. *Chemosphere* **2007**, *68*, 1961−1967.

(98) Nakagawa, Y.; Izumi, K.; Oikawa, N.; Sotomatsu, T.; Shigemura, M.; Fujita, T. *Environ. Toxicol. Chem.* **1992**, *11*, 901−916.

(99) Mackay, D.; Shiu, W.-Y.; Ma, K.-C.; Lee, S. C. *Handbook of Physical-Chemical Properties and Environmental Fate for Organic Chemicals*, 2nd ed.; CRC Press: Boca Raton, FL, 2006; p 4216.

(100) Duffy, E. M.; Jorgensen, W. L. *J. Am. Chem. Soc.* **2000**, *2*, 2878−2888.

(101) Fennell, C. J.; Dill, K. A. *J. Stat. Phys.* **2011**, *145*, 209−226.

(102) Marenich, A. V; Kelly, C. P.; Thompson, J. D.; Hawkins, G. D.; Chambers, C. C.; Giesen, D. J.; Winget, P.; Cramer, C. J.; Truhlar, D. G. *Minnesota Solvation Database*, version 2009; University of Minnesota: Minneapolis, MN, 2009.

(103) Chen, B.; Siepmann, J. I. *J. Phys. Chem. B* **2006**, *110*, 3555−63.

(104) Bhatnagar, N.; Kamath, G.; Chelst, I.; Potoff, J. J. *J. Chem. Phys.* **2012**, *137*, 014502.